TWO NUMERICAL MODELS OF THE SOLIDIFICATION STRUCTURE OF MASSIVE DUCTILE CAST-IRON CASTING

NUMERIČNA MODELA STRUKTURE STRJEVANJA MASIVNEGA DUKTILNEGA ŽELEZOVEGA ULITKA

Karel Stransky[1], Jana Dobrovska[2], Frantisek Kavicka[1], Vasilij Gontarev[3], Bohumil Sekanina[1], Josef Stetina[1]

[1]Faculty of Mechanical Engineering, Brno University of Technology, Technicka 2, 616 69 Brno, Czech Republic
[2]VSB – Technical University of Ostrava, Tr. 17. listopadu, 708 33 Ostrava, Czech Republic
[3]University of Ljubljana, Aškerčeva 12, 1000 Ljubljana, Slovenia
stransky@fme.vutbr.cz

An original three-dimensional (3D) model of solidification is used to describe the process of solidification and cooling of massive (500 × 1000 × 500) mm cast-iron sand moulds castings. The calculated mode of the kinetics of the temperature field of the casting was verified during casting with temperature measurements in selected points.
The sizes and positions (x_i, y_i, z_i, where $i = 1, 2, 3$ is the number of samples taken) of the experimental samples are exactly defined and corresponding with the decreasing rate of solidification. The experimental samples – 15 mm in diameter and 12 mm high – were metallographically analysed and also in terms of heterogeneity of chemical composition. The coordinates x_i, y_i, z_i characterise approximately – within an accuracy of ±5 mm – the centres of the samples. Successively, the local solidification time Θ (i.e. the time the specified position of the casting, defined by the coordinates x_i, y_i, z_i, remained within the temperature range between the liquid and solid curves) is also calculated using the 3 D model. The following dependences are later determined according to experimental and calculated data: the average size of graphite spheroids r_g and of graphite cells R_b as well as the average distances among the particles of graphite L_g – always as function of the local solidification time Θ [x_i, y_i, z_i]. Furthermore, it was founded that the given basic characteristics of the structure of the cast iron r_g, R_b and L_g are directly proportional to the logarithm of the local solidification time. The original spatial model of solidification can therefore be used therefore as first approximation for the assessment of the casting structure of massive cast iron parts. This paper creates the starting point for the estimation of the local mechanical properties and fracture behaviour of massive ductile cast iron castings.

Keywords: ductile cast-iron, solidification time, segregation, structural characteristics, model

Za opis procesa strjevanja in ohlajanja masivnih železovih ulitkov velikosti (500 × 1000 × 500) mm smo uporabili osnovni tridimenzionalni (3 D) model strjevanja. Ulitki so bili uliti v peščene forme. Izračunan kinetični model temperaturnega polja ulitka je bil preverjen med ulivanjem z meritvami temperature v izbranih točkah.
Velikosti in lege (x_i, y_i, z_i, kjer je $i = 1, 2, 3$ število vzetih vzorcev) poskusnih vzorcev so bile točno določene in so v skladu s padajočo hitrostjo strjevanja. Poskusni vzorci premera 15 mm in višine 12 mm so bili metalografsko analizirani in preverjena je bila tudi heterogenost kemijske sestave. Koordinate x_i, y_i, z_i označujejo sredino vzorcev s približno z natančnostjo ±5 mm. Lokalni čas strjevanja Θ (t. j. čas določenega položaja v vzorcu, definiranega s koordinatami x_i, y_i, z_i ostaja v temperaturnem območju med likvidusno in solidusno krivuljo) je bil tudi izračunan z uporabo 3D-modela. Kasneje so bile določene naslednje odvisnosti glede na eksperimentalne in izračunane podatke: srednja velikost kroglastega grafita r_g, grafitnih celic R_b in srednje razdalje med delci grafita L_g – vedno kot funkcije lokalnega časa strjevanja Θ [x_i, y_i, z_i]. Nadalje je bilo ugotovljeno, da so dane značilnosti strukture litega železa r_g, R_b in L_g direktno sorazmerne z logaritmom lokalnega časa strjevanja. Osnovni prostorski model strjevanja lahko tako uporabimo v prvem približku za ugotovitev lite strukture masivnih železovih ulitkov. Ta članek omogoča začetno stopnjo ocene lokalnih mehanskih lastnosti in vedenja pri zlomih masivnih duktilnih železovih ulitkov.

Ključne besede: siva litina s kroglastim grafitom, čas strjevanja, izcejanje, značilnosti strukture, modeliranje

1 INTRODUCTION

The problem of optimisation of properties and production technology for the casting of massive ductile cast-iron (spheroidal graphite) castings had been investigated into in the past few years and, besides an extensive number of publications both nationally as well as internationally, the results of the investigations have been published in the final report of this investigation [1]. During the investigations, the centre of focus were not only the purely practical questions relating to metallurgy and foundry technology, but mainly the verification of the possibility of applying two original models – the 3 D model of transient solidification and cooling of a massive cast-iron casting and the model of chemical and structural heterogeneity. Both models have only been applied to describing the temperature field, the control of solidification and the cooling of continually cast steel slabs, to the descriptions of their chemical heterogeneity and to determining the basic characteristics of their microstructure. The model of chemical and structural heterogeneity seems to be a suitable partner of the 3D model of the transient temperature field [2].

The original model and also an original application of the software ANSYS were one of the outcomes of this research. In this combination, it is possible to optimise the technology of casting cast-iron parts and successive

cooling in order to achieve the most convenient microstructure. This includes a microstructure of spheroids of graphite, preferably with as high a density as possible and spread throughout the casting as evenly as possible, with a minimal ratio of particles of graphite marked as degenerated shapes.

The appropriate density of the spheroids of graphite is simultaneously one of the conditions of good mechanical properties of castings of ductile cast-iron, especially good ductility and contraction while maintaining good strength properties – yield point and tensile strength.

The discussed 3D model establishes a system via which it is possible to pre-simulate the method of eutectic crystallisation of the melt of ductile cast-iron. With the liquidus and solidus known, it is also possible – in selected parts of the casting (that would be suitably discretised) – to determine the time the temperature of the relevant part of the metal remained between the liquidus and solidus. This region is characterised by the coexistence of solid and liquid states – the so-called 'mushy zone'.

In describing the solidification of steel, the time for which the metal remains at a temperature between the liquidus and solidus is called the local solidification time, and the volume of metal corresponding to this time determined by the sizes of the dendrites [3,4]. When describing the solidification of cast-iron, including cast-iron with spheroidal graphite, the term 'local solidification time' has not been used, even despite the fact that the eutectic crystallisation of grey cast-iron always runs within a certain temperature interval and naturally even a time solidification interval dependent on time.

2 AIMS AND METHODOLOGY

The massive experimental cast-iron castings, produced within the research [5], had the following dimensions: width × length × height = (500 × 1000 × 500) mm. The verifying numerical calculation of the local solidification times θ/s – conducted according to the 3D model proved that, along the height, width and length of these massive castings, there are various points with differences in the solidification time of up to two orders.

The aim was to verify the extent to which the revealed differences in the local solidification time affect the following parameters:
a) The average size of spheroidal graphite particles;
b) The average density of spheroidal graphite particles;
c) The average dimensions of graphite cells, and
d) The chemical heterogeneity of elements in the cross-sections of individual graphite cells.

The relationships – among the given four parameters and the corresponding local solidification time – were determined in the series of samples that had been selected from defined positions of the massive casting.

2.1 Experimental cast-iron casting and selection of samples

The experimental casting was selected from a series of three castings and it was marked as casting No.1 [5]. The bottom part of its sand mould was lined with (a total number of) 15 cylindrical chills of a diameter of 150 mm and a height of 200 mm. The upper part of the mould was not lined with any chills. The average chemical composition of the cast-iron before casting is given in **Table 1**.

A (500 × 500 × 40) mm plate had been mechanically cut out of the middle of the length by two parallel transversal cuts. Then, further samples were taken from exactly defined points and tested in terms of their structural parameters and chemical heterogeneity. Samples in the form of testing test-samples for ductility testing, with threaded ends, were taken from the bottom part of the casting (A), from the middle part (C) and from the upper part (G). The 15 mm in diameter and 12 mm high cylindrical samples served the actual measurements in order to determine the structural parameters and chemical heterogeneity.

Table 1: Chemical composition of ductile cast-iron
Tabela 1: Kemijska sestava duktilne železove litine

Element	C	Mn	Si	P	S	Ti	Al	Cr	Ni	Mg
$w/\%$	3.75	0.12	2.15	0.039	0.004	0.01	0.013	0.07	0.03	0.045

Table 2: Measured and calculated structural parameters and the coordinates x, y, z of the measured samples
Tabela 2: Merjeni in izračunani strukturni parametri ter koordinate x, y, z merjenih vzorcev

Sample	$r_g/$ μm	$R_b/$ μm	$L_g/$ μm	$r_{ghm}/$ μm	$R_{bhm}/$ μm	$L_{ghm}/$ μm	$x/$ mm	$y/$ mm	$z/$ mm	$\theta_{ls}/$ s	$\bar{I}_{het}$	$\bar{I}_s$
A	27.6 ± 3.6	82.8	165.6	28	83	110	190	50	507.5	48	0.952	3.34
C	36.4 ± 10.4	103.9	207.7	36	104	136	190	210	507.5	2509	1.091	4.52
G	38.9 ± 12.5	109.3	218.6	39	109	140	190	450	507.5	4542	0.916	3.98

Note: r_g, R_b, L_g – metallographic analysis (measured), r_{ghm}, R_{bhm}, L_{ghm} – chemical micro-heterogeneity (selected for analysis), $L_{ghm} \approx 2R_b - 2r_g$, θ_{ls} – local solidification time, $\bar{I}_{het}$ – arithmetic mean of heterogeneity index, $\bar{I}_s$ – arithmetic mean of segregation index of ten measured elements

In the points of the defined positions of the samples prepared in this way, the quantitative metallographic analysis was used to establish the structural parameters of cast-iron [6], the in-line point analysis to establish the chemical composition of elements [7] and numerical calculation using the 3D model to establish the local solidification time [1].

2.2 Quantitative metallographic analysis

Quantitative analysis of the basic micro-structural parameters in the samples, i.e. the radius of the spheroids of graphite – r_g, the distances between the particles of graphite – L_g and the radius of the graphite cells – R_b had been the subject of a special study [4]. The measurement of the size parameters of the graphite had been conducted on the Olympus CUE4 image analyzer under standard conditions, i.e. with a magnification of 100-times and on each sample a total number of 49 views were evaluated. The measurement results are given in **Table 2**.

2.3 Chemical heterogeneity of samples

The concentration of elements in each of the samples was measured between two particles of spheroidal graphite. The analyzed region in the sample structure had been selected in order for the structural parameters of graphite (r_{ghm}, R_{bhm}, L_{ghm} within the analyzed region) to approach the average parameters of graphite within the sample (r_g, R_b, L_g) measured using quantitative metallo-graphic analysis. The differences of the average values of the parameters in the structures of samples and of para-meters selected for analysis of their chemical micro-heterogeneity of elements are based on the comparison of values in **Table 2**. Then differences occur only between the values of L_g and L_{ghm}, which is given by the fact that parameter L_g represents the average distance between the particles of spheroidal graphite, whereas parameter L_{ghm} represents the measured length of the line between the edges of the graphite within the matrix. This distance was selected in order for the following relation
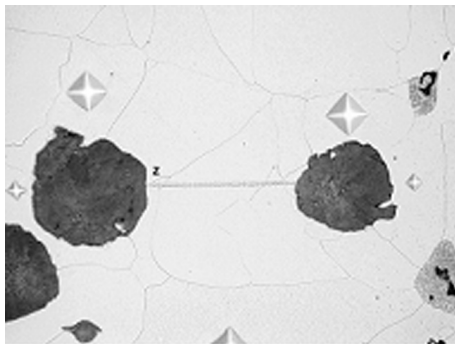

Figure 1: A micro-heterogeneity measurement of ductile cast-iron (the distance between two analysed graphites is 165 μm). Etched by 2 % nital.
Slika 1: Meritve mikroheterogenosti duktilne železove litine (razdalja med dvema analiziranima grafitnima zrnoma je 165 μm). Jedkano z 2-odstotnim nitalom.
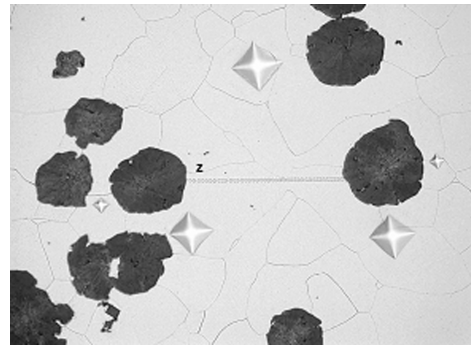

Figure 2: A micro-heterogeneity measurement of ductile cast-iron (the distance between two analysed graphites is 167 μm). Etched by 2 % nital.
Slika 2: Meritve mikroheterogenosti duktilne železove litine (razdalja med dvema analiziranima grafitnima zrnoma je 167 μm). Jedkano z 2-odstotnim nitalom.
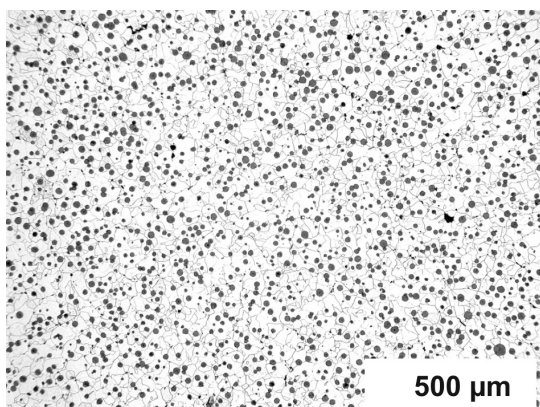
to apply: $L_{ghm} \approx 2R_b - 2r_g$. The actual measurements of concentrations of ten elements – Mg, Al, Si, P, S, Ti, Cr, Mn, Fe, Ni – was carried out on the JEOL – JSM 840/LINK AN 10/85S analytical complex with an energy dispersive X-ray analyzer, an acceleration voltage of the electron beam of 25 kV and exposition time of 50 s. On each of the samples, the concentrations of all ten elements had been measured in three intervals with each individual step being 3 μm. By means of the Neophot light microscope, the interval was documented within which the concentrations were measured. The method of selection of measurement points is illustrated in **Figures 1** and **2** (from the same sample). The results of measure-ments of the chemical heterogeneity of elements in cells were evaluated also statistically with the aim to be able to predict the values of two parameters: the element heterogeneity index I_{het} (which is defined as the quotient of its standard deviation and its arithmetic mean) and the element segregation index I_S (which is defined as the quotient of maximal concentration of elements in the cell and its arithmetic mean).

The results of measurements of the chemical hetero-geneity were evaluated statistically and entered into **Table 3** according to the analysed samples (x is the arithmetic mean of the concentration of the element within the measured interval, I_H is the element hetero-genity index defined as the quotient of its standard deviation and its arithmetic mean, x_{max} is the maximum concentration of the element within the measured inter-val and I_H is the segregation index of the element defined by the quotient $I_S = x_{max} / x$.).

The macrostructure between the bottom and upper part of the massive casting shown in **Figures 3** and **4** was very different. The structure of the bottom of a massive casting is practically without foundry defects (see **Figure 3** and **Table 4** – local solidification time 48 s). On the other hand, in the structure of the upper part of the same casting numerous foundry defects, for example shrink hole, cavities and so on were identified (see **Figure 4** and **Table 4** – local solidification time 4572 s).

Table 3: Results of the chemical heterogeneity measurements – x, x_{max} (w/%), I_H, I_S
Tabela 3: Rezultati merjenj kemijske heterogenosti – x, x_{max} (w/%) I_H, I_S

Sample	r_{ghm} R_{bhm} L_{ghm}	Element									
		Mg	Al	Si	P	S	Ti	Cr	Mn	Fe	Ni
		x I_H x_{max} I_S	x I_H x_{max} I_S	x I_H x_{max} I_S	x I_H x_{max} I_S	x I_H x_{max} I_S	x I_H x_{max} I_S	x I_H x_{max} I_S	x I_H x_{max} I_S	x I_H x_{max} I_S	x I_H x_a $I_{S\,x}$
A	28 83 110	0.0652 0.984 0.201 3.083	0.1002 0.597 0.235 2.345	1.500 0.071 1.676 1.117	0.0151 1.805 0.120 7.947	0.0187 1.377 0.103 5.508	0.0118 1.718 0.068 5.763	0.0615 0.571 0.143 2.325	0.101 0.657 0.242 2.393	97.974 0.002 98.634 1.007	0.156 0.538 0.312 2.000
C	36 104 136	0.0387 1.550 0.260 6.718	0.0620 1.048 0.200 3.226	1.562 0.068 1.841 1.179	0.0151 2.306 0.164 10.861	0.0210 1.539 0.107 5.065	0.0065 2.382 0.061 9.385	0.0615 0.751 0.191 3.106	0.0695 0.815 0.193 2.777	97.981 0.002 98.297 1.003	0.184 0.453 0.349 1.897
G	39 109 140	0.0872 1.138 0.363 4.163	0.0761 0.815 0.216 2.838	1.396 0.076 1.650 1.182	0.0119 1.910 0.085 7.143	0.0282 1.264 0.124 4.397	0.0068 2.314 0.079 11.618	0.0959 0.4867 0.2222 2.315	0.107 0.637 0.283 2.645	98.025 0.002 98.491 1.005	0.166 0.513 0.417 2.512

Figure 3: Macrostructure of the massive ductile iron casting in the bottom part is practically without foundry defects. Etched by 2 % *nital*.
Slika 3: Makrostruktura masovnega duktilnega železovega ulitka na spodnjem delu je praktično brez livnih napak. Jedkano z 2-odstotnim *nitalom*.
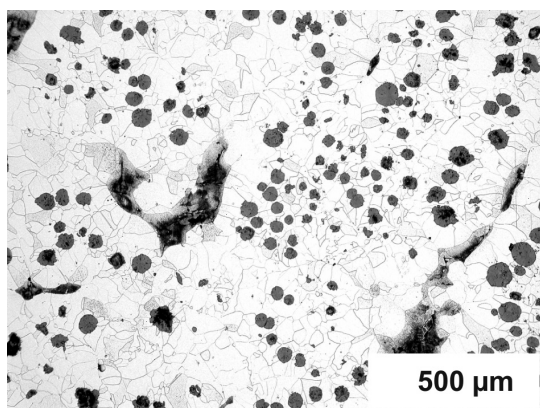
Figure 4: In the macrostructure of the upper part of the same casting is possible to find numerous foundry defects. Etched by 2 % *nital*.
Slika 4: Makrostruktura gornjega dela istega ulitka, kjer je lahko videti številne livne napake. Jedkano z 2-odstotnim *nitalom*.

2.4 Local solidification time

The local solidification times of the selected samples of known coordinates within the casting were calculated using an original in-house 3D model [2] and are given in **Table 2**. The calculation of the liquidus and solidus temperatures for a melt with a composition according to the data in **Table 1**, was performed using special software with the temperature values: 1130 °C (liquidus) and 1110 °C (solidus). The values of the local solidification time θ_{ls} given in **Table 2** therefore relate to the temperature difference between the liquidus and solidus ($\Delta T_{ls} = 20$ °C). If the local solidification time is known, then it is possible to determine the average rate of cooling of the mushy zone as a quotient of the temperature interval and the local solidification time $w_{ls} = \Delta T_{ls} / \theta_{ls} /(°C/s)$.

3 EVALUATION OF RESULTS

It is obvious from the results in **Tables 2 and 3** that in vertical direction from the bottom of the massive casting (sample A: $y = 50$ mm) to the top (gradually samples C: $y = 210$ mm and G: $y = 450$ mm) the characteristic and significant relations are the following:

The average size of the spheroids of graphite, the average size of the cells of graphite and also the average distance between the individual particles of the graphite are all increasing. This relation was confirmed by quantitative metallographic analysis [6].

The chemical heterogeneity within the individual graphite cells is also increasing. The increase in the chemical heterogeneity is reflected most significantly in the increase in the indexes of segregation I_S for magnesium and for titanium, which are increasing in the direction from the bottom of the massive casting to the top in the following order: magnesium $I_S^{Mg} = 3.08$-to-

-6.72-to-4.16; titanium I_S^{Ti} = 5.76-to-9.39-to-11.62 (**Table 3**).

The local solidification time, which increases from the bottom of the casting to the top – from the value of 48 s more than 50-times (near the centre of the casting) and 95-times (at the top of the massive casting), increases very significantly.

The relationships between the structural characteristics of graphite in the casting 2L and the local solidification time were expressed quantitatively using a semi-logarithmic dependence. Despite the fact that, for the structural characteristics of graphite r_{ghm}, R_{bhm} and L_{ghm}, there are only three pairs of measured values, i.e. (r_{ghm},θ_{ls}), (R_{bhm},θ_{ls}) and (L_{ghm},θ_{ls}), the given dependences can be considered significant. As obvious from the research report [6], the quantitative metallographic analysis covers 49 measured views (with a magnification of 100-times) on each of the three 3D samples. This research can therefore be considered as statistically significant.

The relationship between the radius of the graphite spheroids r_{ghm} and the local solidification time θ_{ls}

$$r_{ghm} /\mu m = 19.08 + 2.274 \ln (\theta_{ls}/s) \quad (1)$$

had been found using the least-squares method. The correlation coefficient $r = 0.99$.

Similarly, the relation

$$R_{bhm} /\mu m = 61.33 + 5.567 \ln (\theta_{ls}/s) \quad (2)$$

was established between the radius of the graphite cells and the local solidification time – with a correlation coefficient of $r = 1.00$, and also between the average distance of graphite particles and the local solidification time there is the relation

$$L_{ghm} /\mu m = 84.50 + 6.586 \ln (\theta_{ls}/s) \quad (3)$$

As far as chemical heterogenity of the measured elements is concerned, an analogous relation was established only for the dependence of the segregation index of titanium on the local solidification time, which has a steadily increasing course from the bottom of the casting (sample A) all the way up to the top (sample G). The relevant relation was expressed in the form of a logarithmic equation:

$$\ln I_S^{Ti} /\mu m = 1.201 + 0.1410 \ln (\theta_{ls}/s) \quad (4)$$

where $r = 0.96$.

4 DISCUSSION

The local solidification time θ naturally affects the mechanical properties of cast-iron, however with regard to the dimensions of the test pieces, it is not possible to assign the entire body a single local solidification time. The samples for the testing of tensile strength were taken from the test-sample of the experimental casting in such a way that one had been taken from under the metallographic sample and the second was taken from above. In

this way, the test-samples from along the entire height of the massive casting had been taken and marked: (1A2), (3C4) and (6G7). For example, according to the marking (3C4) test-sample 3 was to be found in experimental casting beneath the metallographic sample C and test-sample 4 above it. The mechanical values determined on these test-samples are arranged in **Table 4**. The last column contains the local solidification times relating to samples A, C and G.

Table 4: Mechanical properties of the samples from experimental casting
Tabela 4: Mehanske lastnosti eksperimentalno ulitih vzorcev

Test-sample		Yield point $R_{p0.2}$/MPa	Tensile strength R_m/MPa	Ductility A_5 /%	Local solidification time* θ_{ls}/s
(1A2)	1	262	388	21.4	48
	2	260	392	24.6	
(3C4)	3	261	394	20.6	2509
	4	266	390	19.4	
(6G7)	6	260	391	14.0	4572

Note: *) metallographic samples A, C, G

Table 4 indicates that in this case the local solidification time θ_{ls} does not affect the yield point $R_{p0.2}$ and the tensile strength R_m of the ductile cast-iron, however, it has significant influence on the ductility A_5. In terms of analytical approximation, the following relationship between the ductility and the local solidification time applies:

$$A_5/\% = 23.399 – 8.1703 (\theta_{ls}/h) \quad (5)$$

where $r = 0.91$. Simultaneously, it could be stated that for four degrees of freedom, which, according to **Table 4**, characterise the six statistically processed pairs (ductility, local solidification time), the correlation coefficient for this level of reliability is 0.917 [8]. In Eq. (5) the ductility is expressed in percentage and the local solidification time in hours. The equation indicates that the reduction in ductility of cast-iron in the state immediately after pouring is – in the first approximation – directly proportional to the square of the local solidification time.

5 CONCLUSION

It can be seen from previous experimentation and the evaluations of the results that led to equations (1) to (5) that – in the general case of the solidification of ductile cast-iron – there could be a dependence of the size of the spheroids of graphite, the size of the graphite cells and therefore even the distance among the graphite particles on the local solidification time, i.e. on the solidification time in which the considered point remains within the *mushy zone*. The described connection with the 3D model of a transient temperature field, which makes it possible to determine the local solidification time, seems to be the means via which it is possible to estimate the

differences in structural characteristics of graphite in cast-iron and also the effect of the local solidification time on ductility in the poured casting. It is known that, for example, the density of spheroids of graphite also significantly influences the mechanical properties of cast-iron, especially contraction and ductility, where the influence of the local solidification time on ductility has been verified (**Equation 5**).

The application of the 3D model of the temperature field, together with the known and experimentally and quantitatively verified relation of microstructural characteristics of cast-iron, could become an effective tool for verifying the above relations in cases comprising complex and massive cast-iron castings.

6 REFERENCES

[1] Kavicka, F. et al.: Optimization of the properties and the technology of the production of massive cast-iron castings. Final Research Report for the GAČR Project No. 106/01/1164. VUT-FSI, Institute of Power Engineering, Brno 2003, 68 pages

[2] Dobrovska J., Kavicka F., Stetina J., Stransky K., Heger J.: Numerical models of the temperature field and chemical heterogenity of a concast steel slab. *Proceedings of the 21st Canadian Congress of Applied mechanics CANCAM 2007*, Toronto, Ontario, Canada, June 2007, 384–385

[3] Smrha, L.: Solidification and crystallisation of steel ingots. SNTL, Prague 1983, 305 pages

[4] Chvorinov, N.: *Crystallisation and heterogeneity of steels*. NČSAV, Prague 1954, 381 pages

[5] Kavicka F., Sekanina B., Stetina J., Stransky K., Gontarev V., Dobrovska J.: Numerical optimization of the method of cooling of a massive casting of ductile cast-iron. Materiali in tehnologie/Materials and technology 43 (**2009**) 2, 73–78

[6] Belko, J., Stransky, K.: Analysing Graphite in Cast-iron. Research Report (611–57, 811–28) VTUO Brno, Brno, November 2002

[7] Winkler, Z., Stransky, K.: Heterogeneity of the Compositions of Elements in Ductile Cast-iron Castings. Research Report (811-11-02) VTÚO Brno, Brno, December 2002

[8] Murdoch, J., Barnes, J. A. Statistical Tables for science, engineering, management and business studies. Macmillan, Cranfield 1970, 40 pages